

**GRAVEL-MANTLED AEOLIAN BEDFORMS FROM MONO-INYO DOMES, CALIFORNIA, USA: MORPHOLOGY, CHARACTERISTICS, AND RELEVANCE TO MARS.** S. P. Scheidt<sup>1</sup> and J. R. Zimbelman<sup>2</sup>, <sup>1</sup>Lunar and Planetary Laboratory, University of Arizona, 1629 E University Blvd, Tucson, AZ 85721 (scheidt@lpl.arizona.edu), <sup>2</sup>CEPS/NASM, Smithsonian Institution, Washington, DC 20013.

**Introduction:** Detailed observations of transverse aeolian ridges (TARs) [e.g., 1] have been obtained by the High Resolution Imaging Science Experiment (HiRISE) camera onboard the Mars Reconnaissance Orbiter (MRO). However, the particle size distribution of the sediments—an important factor in their classification and transport modeling—is below the resolution of the instrument, and only a few direct observations of the sediments have been made from rovers on Mars [e.g., 2]. The study of terrestrial aeolian bedform morphologies on Earth is therefore important for revealing differences in scale, grain-size, and sediment composition. This information can be linked to the physical conditions and processes that create similar shapes on other planetary bodies in the Solar System. However, linkages between the particle-size distribution and the morphology of terrestrial analogs are still not clear. For example, TARs have similar morphology to both reversing sand dunes and gravel-mantled (GM) ripples on Earth [3-4], and may be composed of dust, sand, and/or gravel [5].

Aeolian bedforms on Earth have similar morphology and formation mechanisms, but exhibit substantial variety (e.g., megaripples, granule ripples, and GM ripples [6–12]). Field measurements of topography suggest that GM ripples are an important end-member [3, 4, 10, 11]. They are generally rare on Earth, limited to locations where extremely high velocity wind events interact with loose, unconsolidated materials on the surface in a dry climate. The largest aeolian GM ripples on Earth have been observed in the Puna Desert of Argentina, which are composed of large gravel-sized clasts that accumulate at the crest due to ballistic creep and deflation processes [3]. However, other endmembers at different scales exist, such as in Askja, Iceland, and Mono Lake, CA [12,13].

We have investigated GM ripple fields at the summits of Mono-Inyo Domes, CA (Fig. 1) because previous work has minimally characterized their morphology. The first documented observations of the GM ripples at Mono Domes was in 1981 for South Mono Dome (37.864°N, 119.007°W, 2770 m a.m.s.l.) south of Crater Mountain [14,15]. These fields of GM ripples are distinctly concentrated at high elevation summits where pyroclastic material accumulated during different eruption phases of the greater Mono-Inyo crater/dome chain within Long Valley caldera. These ripples have a wavelength of  $6 \pm 2$  m and an amplitude

of 30–50 cm. The site was revisited in 2003, and ripples were found to be virtually unchanged [16].

Here, we report preliminary observations of previously undocumented groups of high elevation GM ripples observed on North Dome, north of Crater Mountain (37.884°N, 119.006°W, 2687 m a.m.s.l.) from remote sensing, field observation and microtopography derived by multi-view stereo-photogrammetry (MVSP) [e.g., 17]. Undocumented ripples can also be seen from remote sensing at the top of White Wing Mountain (37.726°N, 119.045°W, 3345 m a.m.s.l.), 17 km south of Crater Mountain.



**Figure 1.** Field image showing gravel-mantled (GM) ripples at the summit of North Dome. Red arrows indicate two markers in the background, 8 m apart.

**Field Work and Methods:** Image data and Digital Terrain Models (DTMs) are currently our best resources for studying and comparing aeolian bedform morphologies on Earth and other planetary surfaces. The ripple field at the summit of North Mono Dome was visited on July 29, 2014. Several thousand high-resolution, oblique, field-scale images were taken using a Nikon D7100 along two transects perpendicular to the crests of GM ripples, marked and surveyed by tape measure, Global Positioning System (GPS) and a Brunton compass. The images were processed by MVSP software to create color 3-Dimensional (3D) models of the ground surface that are scaled, georeferenced and of high detail (< 2 mm spatial resolution) [18]. These 3D models show the bedform morphology, the gravel's spatial distribution, particle-size distribution and composition. A trench was dug perpendicular through a GM ripple crest to see the near

surface stratigraphy and was digitized at a 0.3 mm spatial resolution (Fig. 2).

**Results and Discussion:** Mono-Inyo Dome gravel-mantled ripples are similar to those reported in [3,9–11], but are smaller in amplitude and wavelength, younger, less mature and occur at lower elevation and atmospheric pressure. The gravel surface is primarily composed of high albedo (white and gray) low density ( $\rho = 1.7 \text{ g/cm}^3$ ) pumice clasts (1–5 cm in diameter), having a significantly higher fraction on the lee slope of the ripples. The stoss, upwind slope and crest are indicated by higher density ( $\rho = 2.2 \text{ g/cm}^3$ ) low albedo (black) obsidian (Fig. 2), consistent with GM ripples on South Dome [14–16]. It is the alternating light pumice and dark obsidian composition that make the linear bands visible in satellite and aerial images. Ripples on the Mono-Inyo Domes have wavelengths of  $7 \pm 4 \text{ m}$  and amplitudes of 10–50 cm (e.g., Fig. 3).

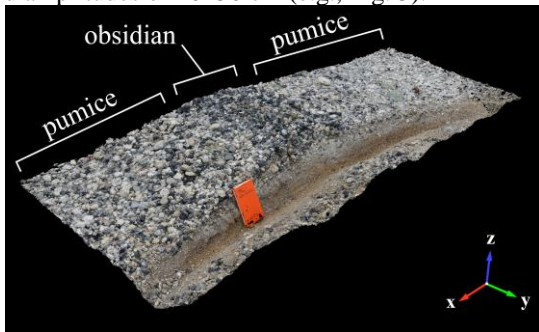


**Figure 2.** 3D model of the trenched GM ripple crest. An orange field book (0.19-m-tall) sits vertically in the trench.

The maximum age of the sediment source for the GM ripples is constrained by the last eruption of the Mono-Inyo Chain between 594–648 A.D. [19], which generated widespread Plinian and phreatomagmatic fall, surge and pyroclastic flow deposits [19]. In a typical stratigraphic section, the eruption produced a complex sequence of gray/white, plinian-type fall beds [19]. The trench in the GM ripple crest on North Dome appeared to lack this sequence, and potentially represents a significant amount of deflation of fine-grained material. The basal Orange-Brown bed unit [19] was encountered < 0.18 m below the surface of the trench,

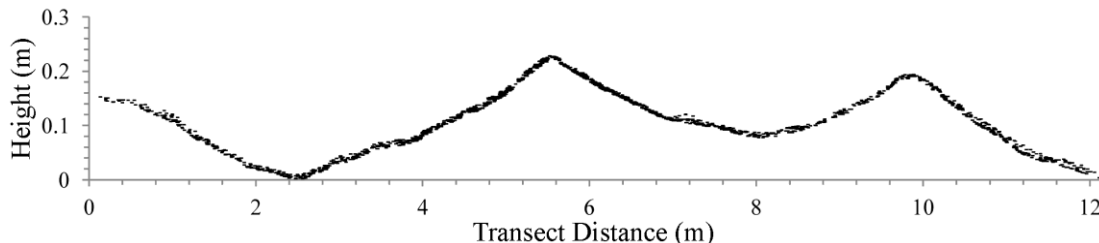


**Figure 3.** Topographic profiles were extracted from MVSP data perpendicular to the crests of gravel-mantled ripples. 3D points are plotted here from a 0.05 m wide region of interest along the transect. Vertical Exaggeration =  $\times 10$ .

superposed by a thin layer of mixed ash and mm-sized pumice clasts between 8–15 cm depth. The uppermost gravel layer, a coarse lag deposit, is free of fines.

**Relevance to Mars:** Fieldwork on a range of terrestrial analog sites is critical to linking climatic, environmental and wind conditions present at the time of formation on Earth or Mars. The Mono-Inyo GM ripples are composed of similar volcanic material that mantles the ripples on the nearby South Dome. They likely share similar aeolian post-modification processes, but at different stages of evolution, as other Mars analog sites in the Puna Desert [3] and Askja [12]. We propose these GM ripples are an important site for comparison of morphological field data to older and larger ripples in the Puna and HiRISE data of TARs on Mars. This site is a good candidate for measuring the affect of surface roughness and ripple topography on the wind [4], which would have important implications for understanding atmospheric boundary conditions on Mars.

**References:** [1] Bourke M.C. et al. (2010) *Geomorphology*, 121, 1–14. [2] Sullivan R. et al. (2007) *LPSC XXXVIII*, Abs. #2048. [3] de Silva S.L. et al. (2013) *Geol. Soc. Amer. Bull.*, 125(11–12), 1912–1929. [4] Zimbelman J.R. and Scheidt S.P. (2014) *Icarus*, 230, 29–37. [5] Geissler P.E. (2014) *JGR—Planets*, 119, doi:10.1002/2014JE004633. [6] Bagnold R.A. (1951) *Brit. J. Appl. Phys.*, 2, 2–29. [7] Sharp R.P. (1963) *J. Geology*, 617–636. [8] Zimbelman J.R. et al. (2012) *Earth Surf. Proc. Land.*, 37, 120–1125. [9] Milana J.P. (2009) *Geology*, 37(4), 343–346. [10] de Silva, S.L. et al. (2014) *LPSC XLV*, 45, Abs. #2582. [11] Zimbelman J.R. et al. (2014) *LPSC XLV*, 45, Abs. #1359. [12] Mountney N.P. et al. (2004) *Sed. Geology*, 166, 3, 223–244. [13] Edgett et al. (1993) *J. Arid.*, 25, 3, 271–297. [14] Greeley R. and Peterfreund A.R. (1981) *Geol. Soc. Amer.* 13(7), 463. [15] Peterfreund A.R. (1982). *11th Int. Cong. Sed.*, 65. [16] Williams S.H. et al. (2003) *Geol. Soc. Amer.*, 35, 265. [17] Wu C. (2011) *VisualSFM: A visual structure from motion system*. [18] Scheidt et al. (2014) *LPSC XLV*, 45, Abs. #1446. [19] Bursik M. et al. (2014) *J. Volcanol. Geotherm. Res.*, 275, 114–131.